REPORT DOCUMENTATION PAGE

Form Approved
OMB No. 0704-0188

1. REPORT DATE *(DD-MM-YYYY)*	2. REPORT TYPE	3. DATES COVERED *(From - To)*
6/21/2018	Final Technical	4/01/2015 - 3/31/2018

4. TITLE AND SUBTITLE
Separation of Internal Waves and Vortical Motions: Analysis of LatMix EM-APEX Float Measurements

5a. CONTRACT NUMBER

5b. GRANT NUMBER
N00014-15-1-2184

5c. PROGRAM ELEMENT NUMBER

6. AUTHOR(S)
Ren-Chieh Lien

5d. PROJECT NUMBER

5e. TASK NUMBER

5f. WORK UNIT NUMBER

7. PERFORMING ORGANIZATION NAME(S) AND ADDRESS(ES)
University of Washington – Applied Physics Laboratory
4333 Brooklyn Avenue NE
Seattle, WA 98105-6613

8. PERFORMING ORGANIZATION REPORT NUMBER

9. SPONSORING / MONITORING AGENCY NAME(S) AND ADDRESS(ES)
Office of Naval Research
875 North Randolph Street
Arlington, VA 22203-1995

10. SPONSOR/MONITOR'S ACRONYM(S)
ONR

11. SPONSOR/MONITOR'S REPORT NUMBER(S)

12. DISTRIBUTION / AVAILABILITY STATEMENT:

Distribution Statement A: Approved for public release; distribution is unlimited.

13. SUPPLEMENTARY NOTES

14. ABSTRACT

Estimates of all terms of potential vorticity (PV) as well as horizontal divergence are computed using float measurements averaged over horizontal scales of O(4–8 km). PV is dominated by its linear components — the vertical relative vorticity (ζ_z) and vertical vortex stretching ($f\,\partial_z\eta$). Both linear components have a rms value of ~0.15 f. In the internal wave frequency band, between f and 0.1 cph, they are coherent and in phase, suggesting the dominance of linear internal waves. A two-dimensional spectrum reveals that PV is dominant at subinertial frequencies and at low vertical wavenumbers. The PV frequency spectrum exhibits a –1 spectral slope with a peak at the inertial frequency. The theoretical prediction of a negative correlation between vertical vorticity and vortex stretching for the linear vortical mode, i.e., reinforcing PV, is confirmed at subinertial frequencies. The linear vortical mode has a Burger number of ~0.8. The estimated linear vortical mode energy spectrum is nearly two orders of magnitude less than the observed total energy spectrum.

15. SUBJECT TERMS
Internal Wave, Vortical Mode, Potential Vorticity, Vertical Vorticity, Horizontal Divergence, Vertical Strain, Burger Number, Small Scale, EM-APEX Float

16. SECURITY CLASSIFICATION OF: a. REPORT	b. ABSTRACT	c. THIS PAGE	17. LIMITATION OF ABSTRACT	18. NUMBER OF PAGES	19a. NAME OF RESPONSIBLE PERSON
Unclassified	Unclassified	Unclassified	UU	12	Ren-Chieh Lien
					19b. TELEPHONE NUMBER *(include area code)* (206) 543-1300

Separation of Internal Waves and Vortical Motions: Analysis of LatMix χ-EM-APEX Float Measurements

Ren-Chieh Lien
Applied Physics Laboratory
University of Washington
1013 NE 40th Street
Seattle, Washington 98105
Phone: (206) 685-1079 fax: (206) 543-6785 email: lien@apl.washington.edu

Thomas B. Sanford
Applied Physics Laboratory and School of Oceanography
University of Washington
1013 NE 40th Street
Seattle, Washington 98105
Phone: (206) 543-1365 fax: (206) 543-6785 email: sanford@apl.washington.edu

Award Number: N00014-15-1-2184

LONG-TERM GOALS

Our long-term scientific goals are to understand the dynamics and identify mechanisms of small-scale processes — i.e., internal tides, inertial waves, nonlinear internal waves, vortical modes, and turbulence mixing — in the ocean and thereby help develop improved parameterizations of mixing for ocean models. Mixing within the stratified ocean is a particular focus, because the complex interplay of internal waves from a variety of sources and turbulence makes this a current locus of uncertainty. Our focus is on observing processes that lead to lateral mixing of water properties.

OBJECTIVES

Our primary scientific objective is to use an innovative swarm of autonomous profilers to improve our understanding and parameterization schemes of small- to submeso-scale oceanic processes. Dispersion due to lateral processes with vertical and horizontal shears could enhance turbulent mixing. Both internal waves and vortical motions exist at vertical scales smaller than order of 10 m and horizontal scales smaller than a few km. They have distinct kinematics and dynamics. Internal waves propagate and may carry energy to remote regions before they break and dissipate via turbulent processes, whereas vortical motions do not propagate and are often long lived. Separation of these two motions is necessary to improve parameterization schemes. Our specific scientific goals for this project are (1) to quantify potential vorticity, relative vorticity, and vortex stretching, and (2) to separate energy of internal waves and vortical motions. Our ultimate goal is to improve our understanding of the effects of internal waves and vortical motions on horizontal dispersion and diapycnal mixing. The first step toward this goal is to separate internal waves and vortical motions and quantify their energy and spectral properties.

ACCOMPLISHMENT UNDER GOALS

We study the internal wave background, shear vector, vorticity vector, and turbulent mixing using measurements taken by a "swarm" of 20 EM-APEX profiling floats in the Sargasso Sea. Ten floats were equipped with a pair of FP07 sensors to measure turbulent thermal dissipation rates. EM-APEX floats profile simultaneously through the surface mixed layer and upper seasonal pycnocline every hour (Fig. 1). These 3-D observations of turbulence, instability, and small-scale processes are vital to understanding the dynamics of the coupling between the diapycnal mixing and oceanic lateral processes.

Floats were deployed three times during the experiment from R/V Endeavor (Fig. 2): Deployment 1 (D1) was conducted during 4–10 June 2011 (collecting 4988 float profiles), Deployment 2 (D2) during 13–16 June 2011 (collecting 2546 float profiles), and Deployment 3 (D3) during 17–20 June 2011 (collecting 2032 profiles). D1 was conducted in a weak straining oceanic regime, and D2 and D3 were conducted in a moderate straining oceanic regime (Shcherbina et al. 2015). Floats were intended to be deployed in three concentric circles of 0.5 km, 1 km, and 2 km radii in the first two deployments, and of 1 km, 2 km, and 4 km radii in the third deployment, with roughly six floats on each circle. However, because of the oceanic horizontal shear, float arrays were not deployed in a perfectly concentric configuration.

Microstructure Capable EM-APEX Floats

Fast responding FP-07 thermistors have been incorporated on autonomous profiling EM-APEX floats to measure microscale ocean temperature fluctuations produced by turbulence. The slow profiling speed of EM-APEX floats enables them to resolve the higher wavenumber regime of the microscale temperature gradient spectrum, beyond the roll-off wavenumber (Fig. 3). The temperature variance dissipation rate χ is computed directly by integrating the observed temperature gradient spectrum over the turbulence wavenumber region without the need to fit the observed temperature gradient spectrum to the empirical spectral form. The accuracy of χ estimated from microstructure EM-APEX floats is confirmed by the agreement, within a factor of 2, between the temperature diffusivity K_T computed from our estimates of χ and estimates of diapcynal diffusivity computed from simultaneous tracer measurements. The observed temperature gradient spectra averaged over many realizations resemble the Batchelor spectral form, though individual spectra often do not fit the empirical prediction. Estimates of χ from different floats have similar temporal fluctuations and vertical profiles, further supporting measurement quality. Estimates of χ exhibit a lognormal distribution, as expected for statistically homogeneous isotropic turbulence (Fig. 4). Turbulence measurements derived from FP-07 sensors on autonomous profiling floats are of comparable quality to those on conventional free-fall microstructure profilers.

Estimates of Small-Scale Potential Vorticity

Observations taken by a swarm of 21 EM-APEX floats, programmed to profile nearly simultaneously, capture the temporal variation and vertical structure of Ertel's potential vorticity (PV). The perturbation PV is defined as

$$PV = \zeta_z - f\partial_z\eta - f cot(\phi)\, \partial_y\eta - \zeta_x\partial_x\eta - \zeta_y\partial_y\eta - \zeta_z\partial_z\eta$$

where ζ_x, ζ_y, and ζ_z are three components of the relative vorticity vector, $\partial_x\eta$ and $\partial_y\eta$ two components of isopycnal slope, $\partial_z\eta$ the vertical strain, $f = 2|\Omega|\sin(\phi)$ the Coriolis frequency, $|\Omega|$ the earth rotation rate, and ϕ the latitude. The first three terms are linear components, whereas the third term is often much smaller than the second term.

Estimates of all terms of PV as well as horizontal divergence are computed using float measurements averaged over horizontal scales of *O*(4–8 km) (Fig. 5). PV is dominated by its linear components — the vertical relative vorticity (ζ_z) and vertical vortex stretching ($f\partial_z\eta$). Both linear components have a rms value of ~0.15 *f*. In the internal wave frequency band, between *f* and 0.1 cph, they are coherent and in phase, suggesting the dominance of linear internal waves (Figs. 6 and 7). Some packets of downward propagating inertial waves exhibit strong vertical vorticity and vortex stretching, > 0.2 *f*. They balance each other closely such that the rms PV, ~0.04 *f*, is less than 20% of the individual components. Vertical vorticity at frequencies > 0.1 cph is contaminated by horizontal divergence due to the unresolved horizontal shear at high horizontal wavenumbers.

A two-dimensional spectrum reveals that PV is dominant at subinertial frequencies and at low vertical wavenumbers (Fig. 8). The PV frequency spectrum exhibits a –1 spectral slope with a peak at the inertial frequency. The PV at near-inertial frequencies is attributed to the differential advection of background PV by low-mode near-inertial waves. Vertical vorticity and vortex stretching are separated into the linear vortical mode and internal wave components following the normal mode decomposition. The theoretical prediction of a negative correlation between vertical vorticity and vortex stretching for the linear vortical mode, i.e., reinforcing PV, is confirmed at subinertial frequencies (Fig. 9). The Burger number of the vortical mode is ~0.8, estimated using the ratio between the vertical vorticity and vortex stretching, implying a quasi-geostrophic flow. The one- and two-dimensional total energy spectrum of the linear vortical mode is computed using the observed PV spectrum and the estimated Burger number. The linear vortical mode energy spectrum is nearly two orders of magnitude less than the observed total energy spectrum (Fig. 10).

IMPACT/APPLICATION

The operation of a swarm of autonomous vehicles simultaneously profiling is a breakthrough advance in the measurement of submesoscale ocean variability. The simultaneity of spatially separated observations eliminates the contamination caused by time differences between sequential observations, the classic scourge of field oceanography. That is, observations at a single site consist of fluctuations caused by both time and space dependencies. Thus, the difference between two observations separated both in time and space contains contributions from both variables. The ability to separate temporal and spatial gradients is a large step forward. Our use of a swarm of AUVs, all programmed to operate in unison, has now demonstrated the advantages over the more traditional methods. During this field study, over 8,000 CTD and velocity profiles were obtained in three experiments.

TRANSITIONS

The EM-APEX float resulted from a SBIR contract from ONR to Webb Research. This instrument has already begun to have an impact on a variety of experiments. The recent ONR DRI projects that the PI has been involved in have EM-APEX components. Other investigators have purchased and used these floats, such as Pete Brodsky, James Girton, Michael Gregg, Jody Klymak (U. Victoria), Eric Kunze, Helen Phillips (U. Tasmania), Zoltan Szuts, and Indian oceanographers. NAVO is reported to be considering purchasing some.

PUBLICATIONS (wholly or in part supported by this grant)

Lien, R.-C. and T. B. Sanford (2018), Small-scale potential vorticity in the upper ocean thermocline, *J. Phys. Oceanogr*., under revision. [submitted]

Lien, R.-C., T. B. Sanford, J. A. Carlson, J. H. Dunlap (2016), Autonomous Microstructure EM-APEX Floats, *Methods in Oceanography*, http://dx.doi.org/10.1016/j.mio.2016.09.003. [published, refereed]

Shcherbina, Y. A. et al. (2015), The LatMix summer campaign: Submesoscale stirring in the upper ocean, A part of the AMS special collection "LatMix: studies of submesoscale stirring and mixing," *Bull. Amer. Meteorol. Soc.*, **96** (8), 1257-1279. DOI:10.1175/BAMS-D-14-00015.1 [published, refereed]

Kunze, E., J. M. Klymak, R.-C. Lien. R. Ferrari, C. M. Lee, M. A. Sundermeyer, and L. Goodman (2015), Submesoscale water-mass spectra in the Sargasso Sea, *J. Phys. Oceanogr*., **45**, 1325-1338. DOI: 10.1175/JPO-D-14-0108.1 [published, refereed]

Sanford, T.B. (2013), Spatial structure of the thermocline and abyssal internal waves, *Deep-Sea Res. Part II.* **85,** 195-209. [published, refereed]

Szuts, Z.B., and T. B. Sanford (2013), Observations of vertically-averaged velocity in the North Atlantic Current, *Deep-Sea Res. Part II.* **85**, 210-219. [published, refereed]

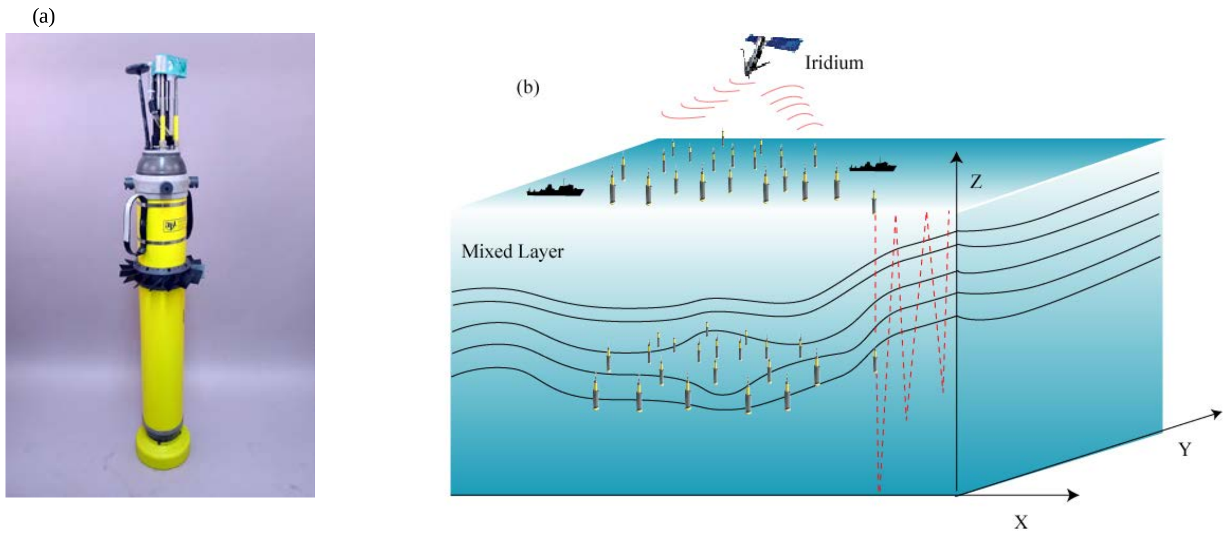

Figure 1: (a) EM-APEX float with dual χ sensors. (b) Schematic of a spatial array of 10 microstructure EM-APEX floats (χ-EM-APEX floats) and 10 regular EM-APEX floats. N.B. The χ sensors were mounted so as to be out of the wake produced by the Iridium antenna, which will be tilted to the side in the so-called "Mai Tai" mounting.

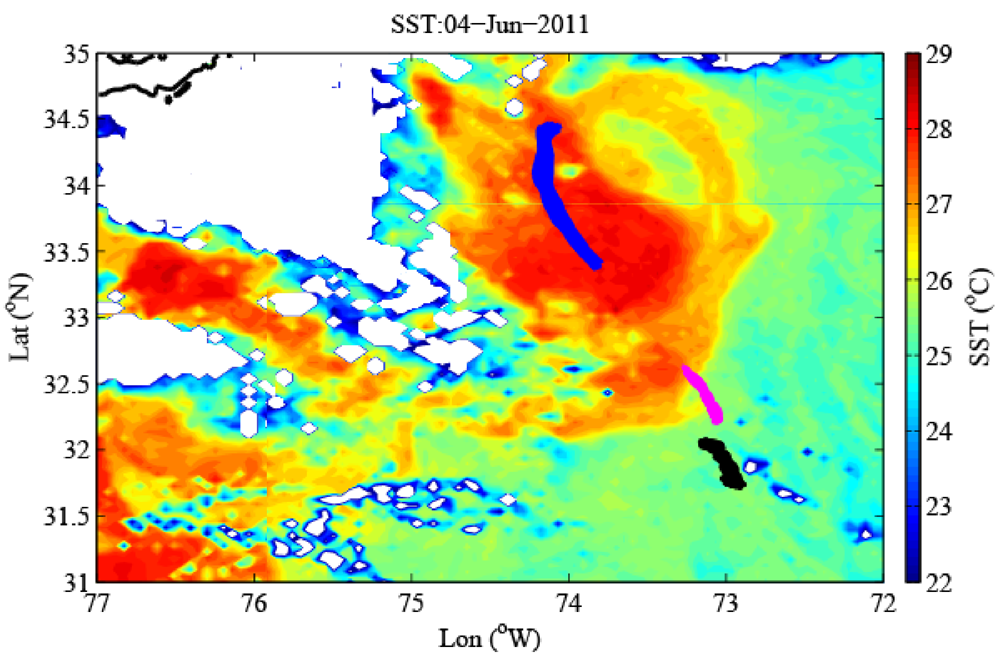

Figure 2: Float trajectories of three deployments during the LatMix experiment. Black curves represent float trajectories on 6–10 June (Deployment 1), pink curves on 13–16 June (Deployment 2), and blue curves on 17–20 June (Deployment 3). Background color shows the AVHRR image of SST on 4 June. The background oceanic condition has a weak strain in Deployment 1, and moderate strain in Deployments 2 and 3.

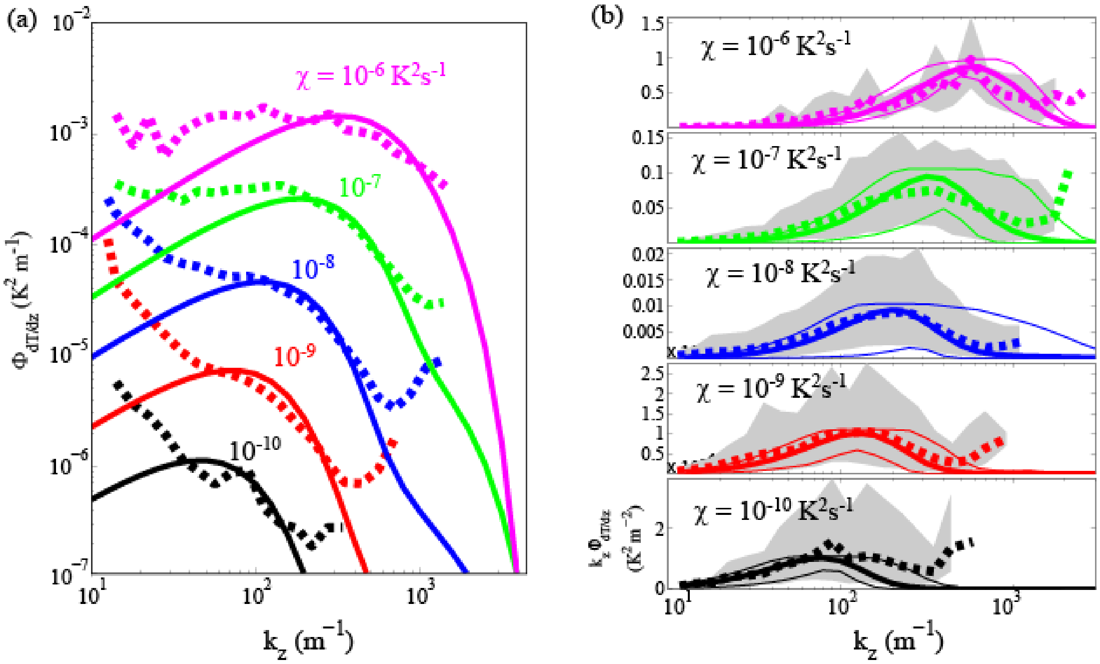

Figure 3: (a) Comparison among observed temperature gradient spectra (dashed) with Batchelor spectra (solid) for χ of $10^{-10} - 10^{-6}$ $K^2 s^{-1}$. (b) Similar to (a) but in variance preserving format. (b) Gray shadings represent 95% confidence interval of observed spectra, and thin curves represent 95% confidence interval of Batchelor spectra.

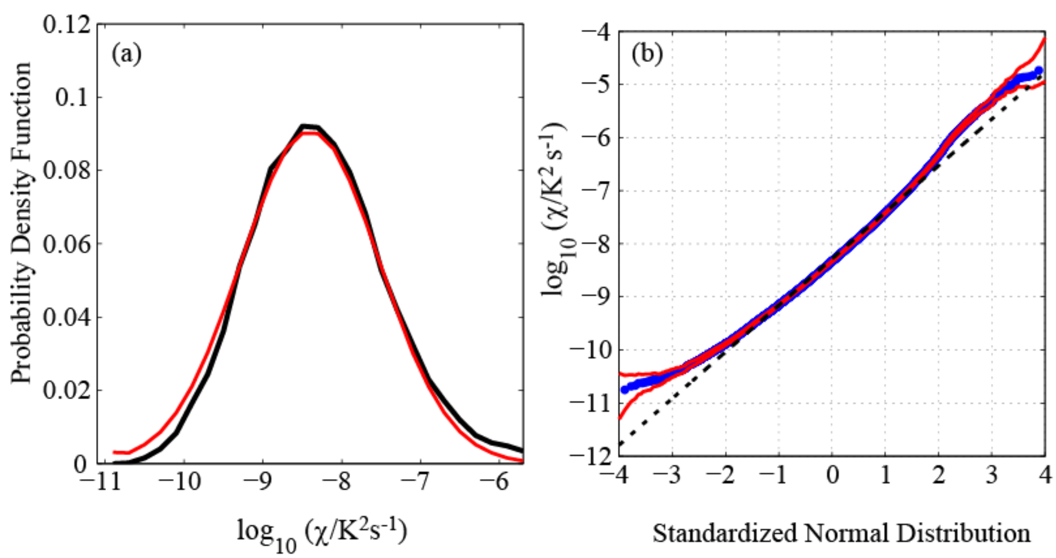

Figure 4: (a) Probability density function of the ensemble of $\log_{10}(\chi)$ observations from all floats (black curve) compared with that expected from a theoretical normal distribution of the observed mean (–8.3) and standard deviation (0.9) (red curve). (b) Q-Q plot of $\log_{10}(\chi)$ vs. that of standardized normal distribution. The blue curve shows observed Q-Q structure. Red curves represent the 95% confidence interval assuming a normal distribution. The black dashed curve represents the theoretical normal distribution.

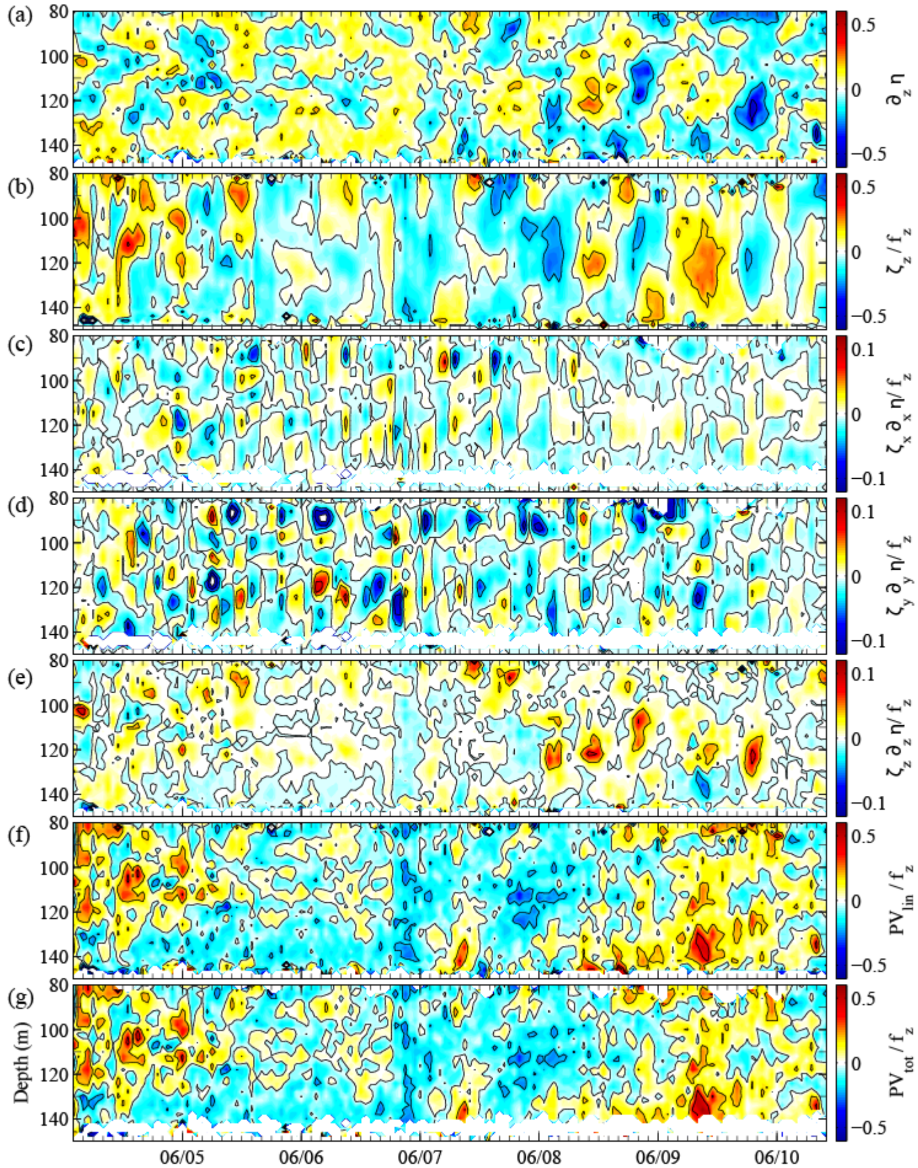

Figure 5: Depth–time variations of normalized PV: (a) vertical strain (normalized vortex stretching), (b) normalized vertical vorticity, (c)–(e) nonlinear components, (f) linear PV, and (g) the sum of linear and nonlinear components of PV. Note that the range of the color scale in panels (c)–(e) is different from other panels to illustrate that the nonlinear components of PV are much smaller than the linear components.

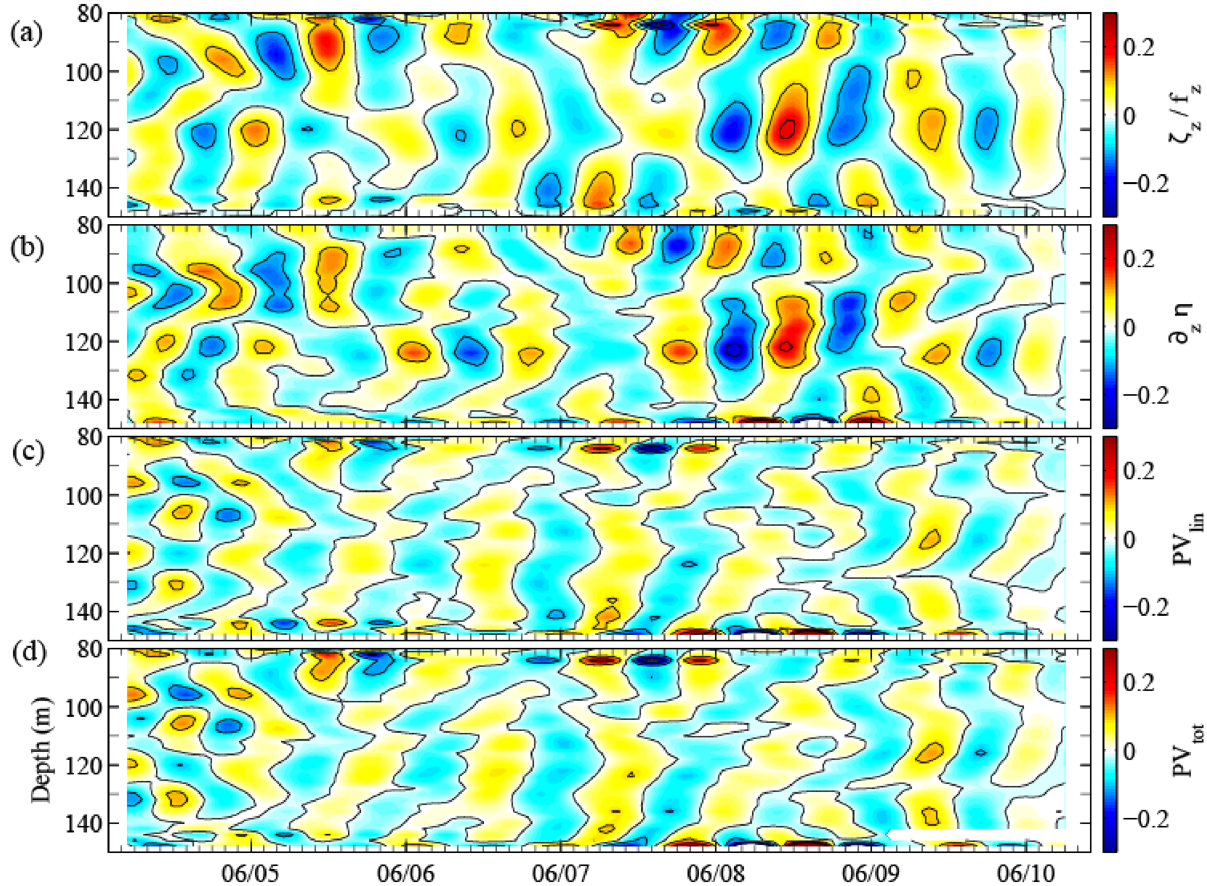

Figure 6: Depth–time variations in the internal wave frequency band of normalized (a) vertical vorticity, (b) vertical strain, (c) linear PV, and (d) total PV. All variables have been band-pass filtered in the internal wave low-frequency band between 0.04 and 0.1 cph.

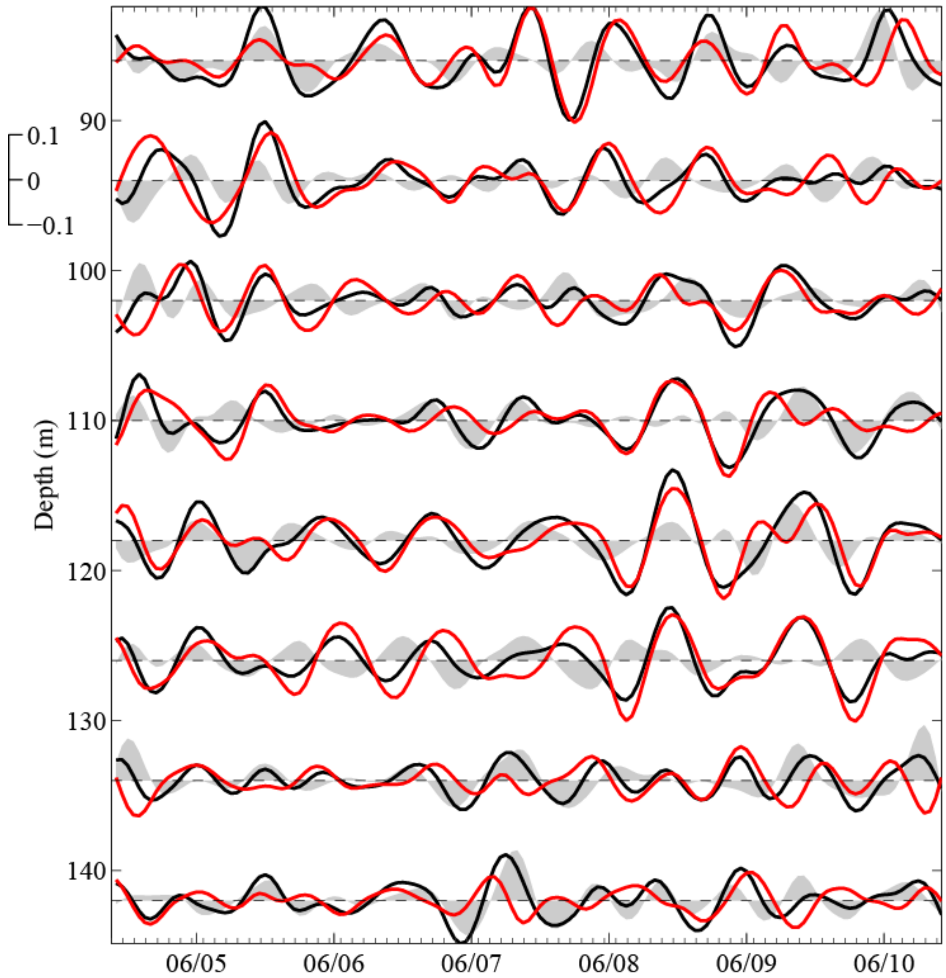

Figure 7: Time series of normalized vertical vorticity (black curve), vertical strain (red curve), and the normalized linear PV (shading) after band-pass filtered between 0.04 and 0.1 cph, within the internal wave low-frequency band, between 84 m and 142 m depth at 8-m intervals. The scale is illustrated at the left side of the panel.

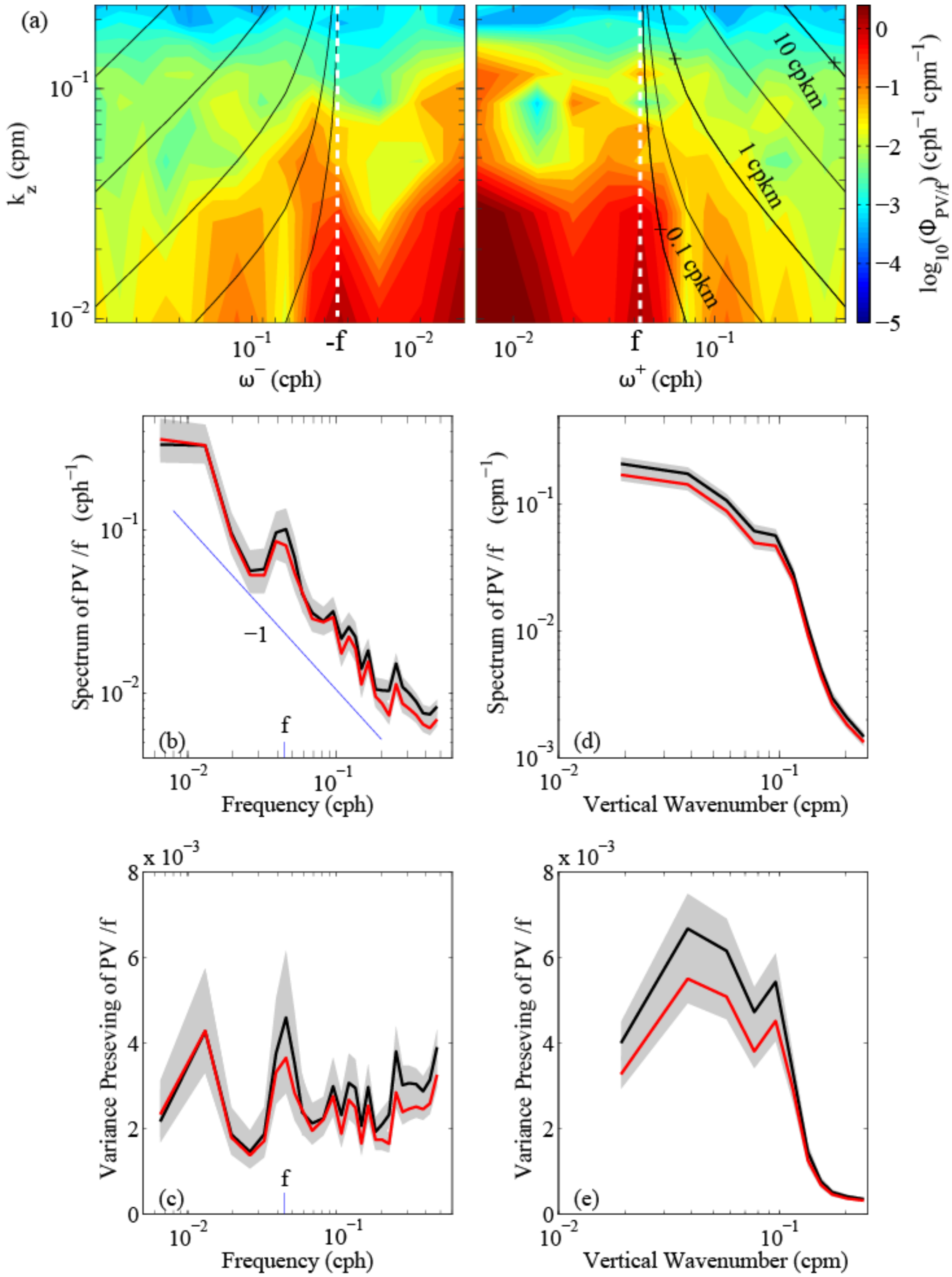

Figure 8: (a) Two-dimensional spectrum, (b) frequency spectrum, (c) variance preserving frequency spectrum, (d) vertical wavenumber spectrum, and (e) variance preserving vertical wavenumber spectrum of normalized PV. The black curve represents the total PV and the red curve the linear component of PV. The blue line in (a) marks a reference –1 spectral slope. In panel (a) white vertical dotted lines mark the inertial frequency. Black contour curves represent constant horizontal wavenumbers as a function of frequencies and vertical wavenumbers for linear internal waves, i.e. the dispersion relation.

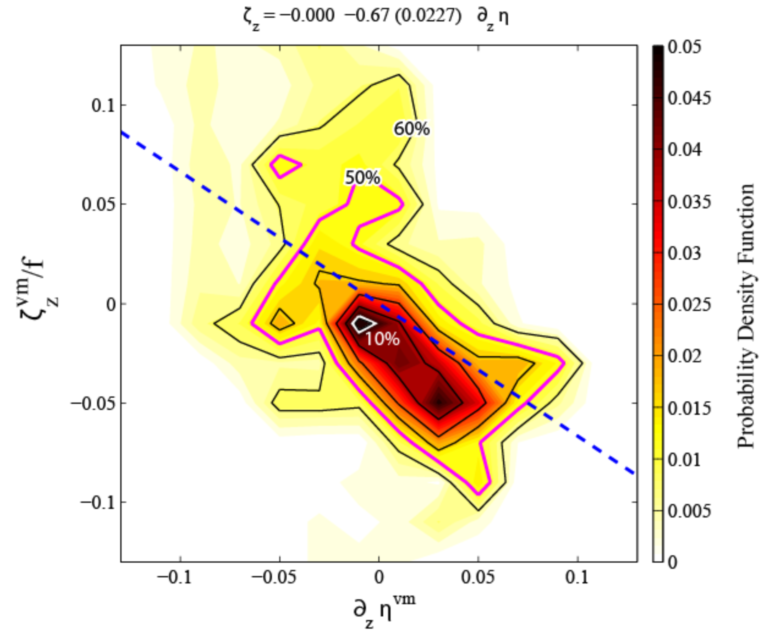

Figure 9：Two-dimensional histogram of vertical vorticity vs. vertical stain of the vortical mode. The color shading shows the probability density function. The white and magenta contour lines mark 10% and 50% of the accumulated occurrence, and black contour lines 20%, 30%, 40%, and 60% of the accumulated occurrence. The blue dashed line shows the linear regression fit.

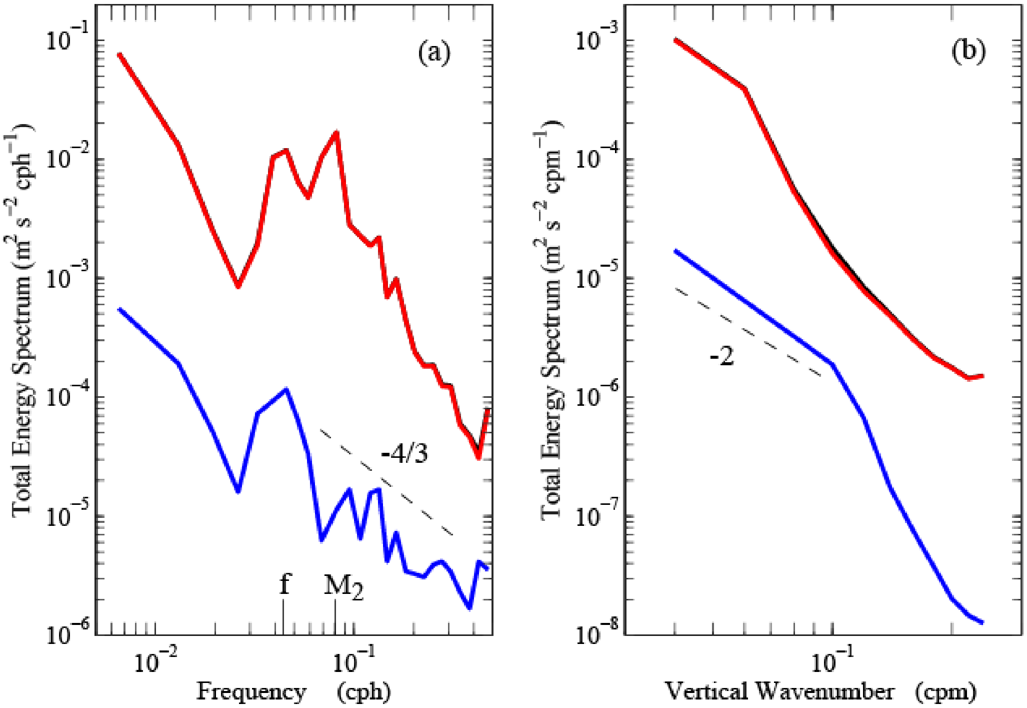

Figure 10: (a) Frequency spectra of total observed energy (red curve) and the linear vortical mode component (blue curve). (b) Vertical wavenumber spectra of total observed energy (red curve) and the linear vortical mode component (blue curve). The dashed lines mark the reference spectral slopes

of –4/3 and –2.